Ubiquitylation of phosphatidylinositol 4-phosphate 5-kinase type I γ by HECTD1 regulates focal adhesion dynamics and cell migration

Xiang Li[1], Qi Zhou[1], Manjula Sunkara[2], Matthew L. Kutys[3], Zhaofei Wu[1], Piotr Rychahou[1], Andrew J. Morris[2], Haining Zhu[4], B. Mark Evers[1] and Cai Huang[1,5,*]

[1]Markey Cancer Center, University of Kentucky, Lexington, KY 40506, USA
[2]Division of Cardiovascular Medicine, Department of Internal Medicine, University of Kentucky, Lexington, KY 40506, USA
[3]NIDCR, National Institutes of Health, Bethesda, MD 20892, USA
[4]Department of Molecular and Cellular Biochemistry, University of Kentucky, Lexington, KY 40506, USA
[5]Department of Molecular and Biomedical Pharmacology, University of Kentucky, Lexington, KY 40506, USA
*Author for correspondence (cai-huang@uky.edu)

Accepted 25 March 2013
Journal of Cell Science 126, 2617–2628

doi: 10.1242/jcs.117044

Summary

Phosphatidylinositol 4-phosphate 5-kinase type I γ (PIPKIγ90) binds talin and localizes at focal adhesions (FAs). Phosphatidylinositol (4,5)-bisphosphate (PIP_2) generated by PIPKIγ90 is essential for FA formation and cell migration. On the other hand, PIPKIγ90 and the β-integrin tail compete for overlapping binding sites on talin. Enhanced PIPKIγ90-talin interaction suppresses talin binding to the β-integrin. It is unknown how PIPKIγ90 is removed from the PIPKIγ90–talin complex after on-site PIP_2 production during cell migration. Here we show that PIPKIγ90 is a substrate for HECTD1, an E3 ubiquitin ligase regulating cell migration. HECTD1 ubiquitinated PIPKIγ90 at lysine 97 and resulted in PIPKIγ90 degradation. Expression of the mutant PIPKIγ90^{K97R} enhanced PIP_2 and PIP_3 production, inhibited FA assembly and disassembly and inhibited cancer cell migration, invasion and metastasis. Interestingly, mutation at tryptophan 647 abolished the inhibition of PIPKIγ90^{K97R} on FA dynamics and partially rescued cancer cell migration and invasion. Thus, cycling PIPKIγ90 ubiquitylation by HECTD1 and consequent degradation remove PIPKIγ90 from talin after on-site PIP_2 production, providing an essential regulatory mechanism for FA dynamics and cell migration.

Key words: HECTD1, PIP5K1C, Metastasis, Invasion, Ubiquitylation

Introduction

Cell migration is a dynamic process that requires focal adhesion (FA) assembly at the front of cells, with concomitant disassembly at the trailing edges of cells (Webb et al., 2002; Ridley et al., 2003). Therefore, FAs are central regulatory points for cell migration.

FAs have been implicated in cancer metastasis. Several molecules, including DRR (Down-Regulated in Renal cell carcinoma), filamin A, focal adhesion kinase (FAK) and paxillin, regulate cancer invasion through modulating FA disassembly (Chan et al., 2010; Le et al., 2010; Xu et al., 2010b; Deakin and Turner, 2011). Also, microarray analysis shows that about one-third of the genes that are induced in metastatic cancers are genes affecting cell adhesion and the cytoskeleton (Clark et al., 2000). Interestingly, paxillin, a FA protein, is involved in FA dynamics in 3D matrix and cancer metastasis (Deakin and Turner, 2011). Many molecules, including FAK, paxillin, talin, calpain, Smurf1 and PAK1 have been shown to regulate FA dynamics (Franco et al., 2004; Webb et al., 2004; Huang, C. et al., 2009; Delorme-Walker et al., 2011). However, the underlying molecular mechanisms are not fully understood.

Phosphatidylinositol 4-phosphate 5-kinase type I γ (PIPKIγ90) is a key enzyme that is responsible for the production of phosphatidylinositol (4,5)-bisphosphate (PIP_2), a molecule that is well implicated in FA formation. PIPKIγ90 interacts with talin and localizes at FAs (Di Paolo et al., 2002; Ling et al., 2002). PIPKIγ90 is essential for FA dynamics (Wu et al., 2011), probably by modulating integrin–ligand binding and integrin–actin force coupling (Legate et al., 2011). PIPKIγ90 regulates cell migration and cancer invasion (Sun et al., 2007; Sun et al., 2010; Wu et al., 2011). It also regulates cell polarization, LFA-1-mediated T cell adhesion as well as adherens junction (Ling et al., 2007; Lokuta et al., 2007; Xu et al., 2010a).

PIPKIγ90 and the β-integrin tail compete for the same binding site on talin (Barsukov et al., 2003; de Pereda et al., 2005). Overexpression of PIPKIγ90 inhibits integrin activation and causes defects in cell spreading and FA formation (Di Paolo et al., 2002; Ling et al., 2002; Calderwood et al., 2004). Phosphorylation of PIPKIγ90 by Src promotes its interaction with talin, inhibiting the talin–β-integrin interaction (Ling et al., 2003), whereas Cdk5-mediated phosphorylation of PIPKIγ90 disrupts PIPKIγ90–talin interaction (Lee et al., 2005). Since the role of Cdk5 in cell migration in many cell types remained to be defined, it is unknown how PIPKIγ90 binds talin to produce on-site PIP_2 but does not inhibit the β-integrin-tail–talin binding, a key step in integrin activation and FA formation in migratory cells. Since Smurf1 ubiquitylates the talin head and is implicated in FA dynamics and cell migration (Huang et al., 2009; Huang,

2010), we originally hypothesized that in migratory cells PIPKIγ90 was ubiquitylated by Smurf1 and consequently degraded upon on-site PIP_2 production. However, we demonstrated that HECTD1, an E3 ubiquitin ligase regulating cell migration (Sarkar and Zohn, 2012), instead of Smurf1, ubiquitylated PIPKIγ90 and caused its degradation. Thus, PIPKIγ90 degradation may withdraw its competition for binding talin, consequently leading to FA assembly/disassembly and cell migration in breast cancer cells.

Results

PIPKIγ90 is ubiquitylated by HECTD1 at lysine 97

To examine whether PIPKIγ is ubiquitylated in breast cancer cells, we treated MDA-MB-157, MDA-MB-231 and MDA-MB-468 cells with carfilzomib plus bortezomib, specific proteasome inhibitors, and observed the steady-state levels of PIPKIγ. Carfilzomib plus bortezomib treatment resulted in a significant increase in the levels of PIPKIγ in MDA-MB-157, MDA-MB-231 and MDA-MB-468 cells (Fig. 1A). The proteasome inhibitors also induced a significant increase in the levels of PIPKIγ in human umbilical vein endothelial cells (HUVEC) and EGFP–PIPKIγ90 stably expressed in Chinese hamster ovary (CHO) K1 cells (supplementary material Fig. S1A). The ubiquitylation of PIPKIγ was further verified by immunoprecipitating PIPKIγ and detecting with an anti-ubiquitin antibody (Fig. 1B). These results suggest that PIPKIγ is regulated by ubiquitylation in a variety of cell types.

To learn which E3 ubiquitin ligase mediates the ubiquitylation of PIPKIγ, we adapted the AviZZ system that we originally developed for protein–protein interaction assays (Huang and Jacobson, 2010). CHO-K1 cells stably expressing BirA, a biotin ligase, were transfected with Avi-ubiquitin and ZZ-PIPKIγ90 with or without different ligases. The cells were labeled with biotin and ZZ-PIPKIγ90 was precipitated with IgG–Sepharose. PIPKIγ90 ubiquitylation was detected by using Dylight680 streptavidin. Transfection with Smurf1 (Smad ubiquitination regulatory factor 1) and Smurf2 resulted in a dramatic increase in the ubiquitylation of PIPKIγ90 (supplementary material Fig. S1B). To examine whether Smurf1 or Smurf2 are the E3 ligases that are responsible for PIPKIγ90 ubiquitylation in breast cancer cells, endogenous Smurf1 and Smurf2 in MDA-MB-231 cells were depleted using shRNA. The cells were treated with DMSO or the proteasome inhibitors. Neither Smurf1 nor Smurf2 shRNA blocked the proteasome inhibitor-induced increase in PIPKIγ90 levels (supplementary material Fig. S1C). Thus, other E3 ligases may be responsible for PIPKIγ90 ubiquitylation in MDA-MB-231 cells, although overexpression of Smurf1 and Smurf2 ubiquitylates PIPKIγ90 in CHO-K1 cells.

HECTD1, an E3 ubiquitin ligase homologous to Smurf1, has been shown to regulate cell migration (Sarkar and Zohn, 2012). To examine whether HECTD1 is the E3 ligase that is responsible for PIPKIγ90 ubiquitylation in breast cancer cells, endogenous HECTD1 in MDA-MB-231 cells was depleted by expressing HECTD1 shRNA. The cells were treated with DMSO or proteasome inhibitors bortezomib plus carfilzomib, and PIPKIγ90 levels were detected by western blotting. HECTD1 knockdown caused an increase in PIPKIγ90 levels and also partially (D6) or completely (D9) abolished the increase in PIPKIγ90 levels induced by proteasome inhibitors (Fig. 1C). To

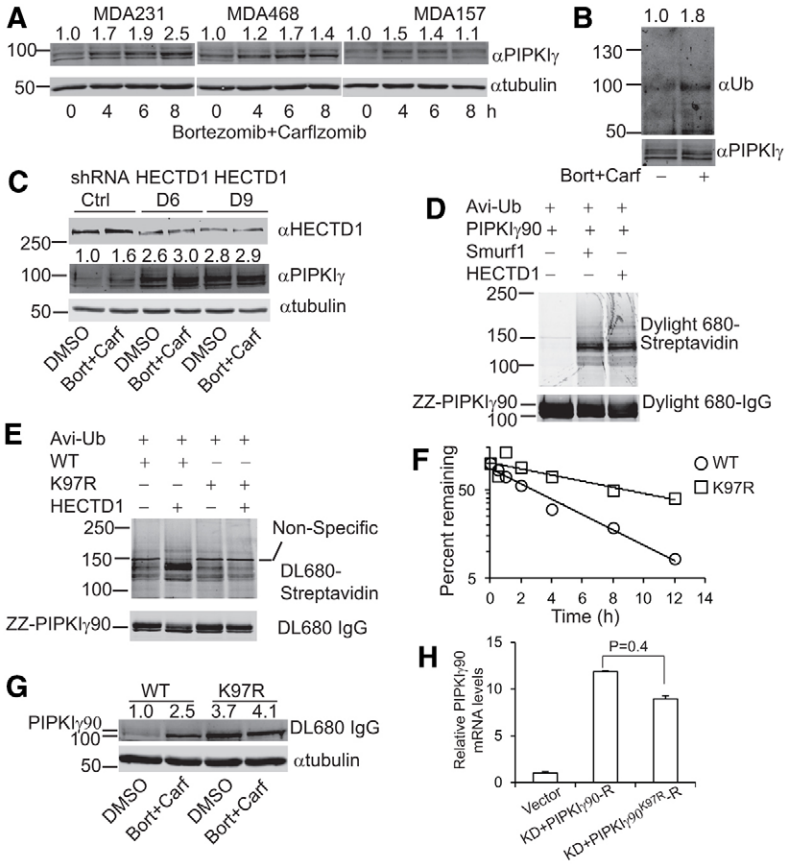

Fig. 1. HECTD1 ubiquitylates PIPKIγ90 at lysine 97. (**A**) The steady-state levels of PIPKIγ were measured by western blotting in MDA-MB-157, MDA-MB-231 and MDA-MB-468 breast cancer cells treated with bortezomib plus carfilzomib (1 μM each) for the times indicated. (**B**) The ubiquitylation of endogenous PIPKIγ was determined by immunoprecipitating PIPKIγ and blotting with an anti-ubiquitin antibody. (**C**) Effect of HECTD1 knockdown on PIPKIγ levels in the absence and presence of proteasome inhibitors. HECTD1 shRNA D6 and D9 were stably expressed in MDA-MB-231 cells by lentiviral infection. (**D**) PIPKIγ90 was ubiquitylated by Smurf1 and HECTD1 in CHO-K1 cells. CHO-K1 cells that stably express BirA were transfected with Avi-ubiquitin and ZZ-PIPKIγ90 with or without different ligases. (**E**) Substitution of lysine 97 with arginine (K97R) abolished HECTD1-mediated ubiquitylation of PIPKIγ90. (**F**) Time course of degradation of PIPKIγ90 and PIPKIγ90^{K97R} in CHO-K1 cells. CHO-K1 cells expressing BirA were transfected with Avi-PIPKIγ90 or Avi-PIPKIγ90^{K97R} and incubated with biotin for 4 hours. The levels of Avi-PIPKIγ90 and Avi-PIPKIγ90^{K97R} were detected by western blotting using Dylight800-Streptavidin. (**G**) The steady-state levels of PIPKIγ90 WT and PIPKIγ90^{K97R} were measured by western blotting in endogenous PIPKIγ-depleted MDA-MB-231 cells expressing ZZ-PIPKIγ90-R or ZZ-PIPKIγ90^{K97R}-R, respectively, and treated with DMSO or bortezomib plus carfilzomib (1 μM each). (**H**) The relative mRNA levels of PIPKIγ90 in MDA-MB-231 cells infected with a shRNA control (Vector; value set to 1.0) and in PIPKIγ-depleted cells expressing PIPKIγ90-R or PIPKIγ90^{K97R}-R. Values indicate mean ± s.e.m. (n=5).

know whether HECTD1 ubiquitylates PIPKIγ90, CHO-K1 cells expressing BirA were transfected with Avi-ubiquitin and ZZ-PIPKIγ90 with Smurf1 and HECTD1. PIPKIγ90 ubiquitylation was measured as described earlier. Both Smurf1 and HECTD1 promoted PIPKIγ90 ubiquitylation in CHO-K1 cells (Fig. 1D). Thus, HECTD1 is responsible for PIPKIγ90 ubiquitylation.

To identify the ubiquitylation sites on PIPKIγ, ZZ-PIPKIγ87 was transfected into CHO-K1 cells and purified with IgG–Sepharose beads. Purified ZZ-PIPKIγ87 (on Sepharose beads) was ubiquitylated *in vitro* and digested with trypsin and chymotrypsin. The peptides were analyzed by LC-MS/MS using an LTQ-Orbitrap mass spectrometer. Since the last three residues at the C-terminus of ubiquitin are Arg-Gly-Gly, trypsin digestion occurs after the arginine residue thus leaving the two glycine residues that are covalently attached to the ubiquitylated peptide. The PIPKIγ peptide ^{95}SSKPER was detected as a ubiquitylated peptide and the tandem MS/MS spectrum clearly showed that the Gly-Gly adduct was on lysine 97 (K97) within the peptide (supplementary material Fig. S2A).

To examine whether K97 is also an ubiquitination site for HECTD1, wild type (WT) ZZ-PIPKIγ90 and ZZ-PIPKIγ90^{K97R} were co-transfected with Avi-ubiquitin with or without HECTD1 into CHO-K1 cells that stably express BirA. The ubiquitylation of the WT and mutant PIPKIγ90 was measured as described above. Mutation at K97 completely abolished HECTD1-mediated ubiquitylation of PIPKIγ90 (Fig. 1E). Similar results were observed in MDA-MB-231 cells expressing the WT and mutant PIPKIγ90^{K97R} (supplementary material Fig. S2B).

To examine whether PIPKIγ90 ubiquitylation causes its degradation, CHO-K1 cells that express BirA were transiently transfected with Avi-PIPKIγ90 or Avi-PIPKIγ90^{K97R}, and then incubated with biotin. The levels of Avi-PIPKIγ90 or Avi-PIPKIγ90^{K97R} at different times after biotin was removed were detected by western blotting using Dylight800 streptavidin. The half-life of PIPKIγ90 was ~3 hours, whereas mutation at K97 tripled its half-life (Fig. 1F). Also, co-transfection of HECTD1 with PIPKIγ90 caused a decrease in the steady-state level of PIPKIγ90, but HECTD1 did not affect paxillin, talin and vinculin (supplementary material Fig. S2C). These results indicate that PIPKIγ90 ubiquitylation by HECTD1 causes its degradation.

To examine whether PIPKIγ90 ubiquitylation also mediate PIPKIγ90 degradation in breast cancer cells, MDA-MB-231 cells were infected with PIPKIγ90 shRNA lentiviral particles to knockdown the endogenous PIPKIγ90, and the cells were further infected with recombinant retroviruses that express codon-modified WT ZZ-PIPKIγ90 (ZZ-PIPKIγ90-R) and ZZ-PIPKIγ90^{K97R} (ZZ-PIPKIγ90^{K97R}-R), respectively. The expression levels of the WT and mutant PIPKIγ90 were determined by western blotting after the cells were treated with DMSO or proteasome inhibitors. The protein level of PIPKIγ90^{K97R} was 2.7 times higher than those of the WT (Fig. 1G). Treatment with bortezomib plus carfilzomib resulted in a 1.5-fold increase in the level of the WT, whereas the mutant PIPKIγ90^{K97R} levels were not further increased by proteosome inhibitors since its degradation is already defective. The mRNA levels between the WT and PIPKIγ90^{K97R} are no different (Fig. 1H). These results confirm that K97 is the ubiquitylation site of PIPKIγ90 and indicate that PIPKIγ90 ubiquitylation leads to its degradation.

To determine whether PIPKIγ90 ubiquitylation modulates PIP_2 and PIP_3 production in breast cancer cells, polyphosphoinositides in PIPKIγ90-depleted MDA-MB-231 cells that express ZZ-PIPKIγ90-R and ZZ-PIPKIγ90^{K97R}-R respectively, and control MDA-MB-231 cells (infected with a control shRNA) were extracted, derivatized using trimethylsilyl diazomethane and measured using mass spectrometry. There was no significant difference in PIP levels among PIPKIγ90-R, PIPKIγ90^{K97R}-R cells and control MDA-MB-231 cells; the control cells and PIPKIγ90-depleted cells that express PIPKIγ90-R had similar PIP_2 and PIP_3 levels. However, the cells that express PIPKIγ90^{K97R}-R demonstrated much higher PIP_2 and PIP_3 than the control cells (Fig. 2A). Also, mutation at K97 had no significant effect on PIPKIγ90 activity as both WT protein and K97R mutant showed similar kinase activity in the *in vitro* assay (Fig. 2B). These results indicate that PIPKIγ90 ubiquitylation is a novel regulatory mechanism for phosphoinositide metabolism.

PIPKIγ90 ubiquitylation is required for efficient FA turnover in breast cancer cells

We have demonstrated that PIPKIγ90 regulates FA dynamics in CHO-K1 and HCT116 cells (Wu et al., 2011). Since E3 ubiquitin ligases have been implicated in regulating FA dynamics (Huang et al., 2009; Huang, 2010), we determined whether PIPKIγ90 ubiquitylation influences FA assembly/disassembly. MDA-MB-231 cells that stably express DsRed-paxillin were infected with retroviruses that express ZZ-PIPKIγ90 or ZZ-PIPKIγ90^{K97R} (Fig. 3A). The cells were plated on MatTek dishes (with a glass coverslip at the bottom) precoated with fibronectin (5 μg/ml) and TIRF images of DsRed-paxillin were taken using a Nikon TIRF microscope. Images were recorded at 1-minute intervals for a 60-minute period. FA assembly and disassembly rate constants were calculated as we described previously (Huang et al., 2009; Wu et al., 2011). FA assembly/disassembly rates in

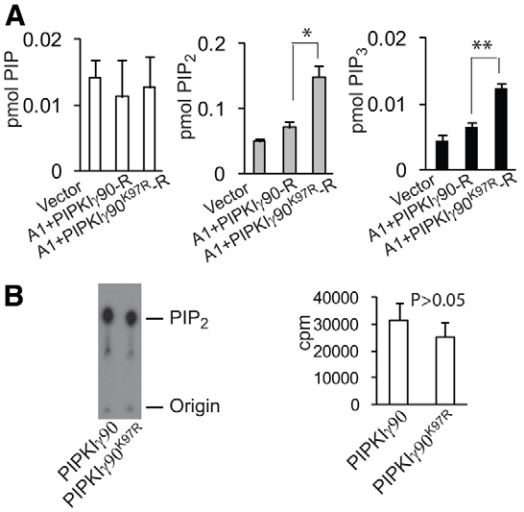

Fig. 2. PIPKIγ90 ubiquitylation regulates PIP_2 and PIP_3 production. (**A**) Phosphoinositide levels in MDA-MB-231 cells expressing a shRNA control (Vector) and in PIPKIγ-depleted MDA-MB-231 cells expressing ZZ-PIPKIγ90-R or ZZ-PIPKIγ90^{K97R}-R (n=4). (**B**) Substitution of lysine 97 with arginine did not affect PIPKIγ90 activity *in vitro*. ZZ-PIPKIγ90 and ZZ-PIPKIγ90^{K97R} were immunoprecipitated using IgG-Agarose beads. The beads were incubated with PI(4)P and [γ-^{32}P]ATP, and PIP_2 production analyzed with TLC. PIP_2 was visualized by autoradiography (left panel) and quantified by liquid scintillation counting (right panel). Data are means ± s.e.m. of three independent experiments.*P<0.05, **P<0.01.

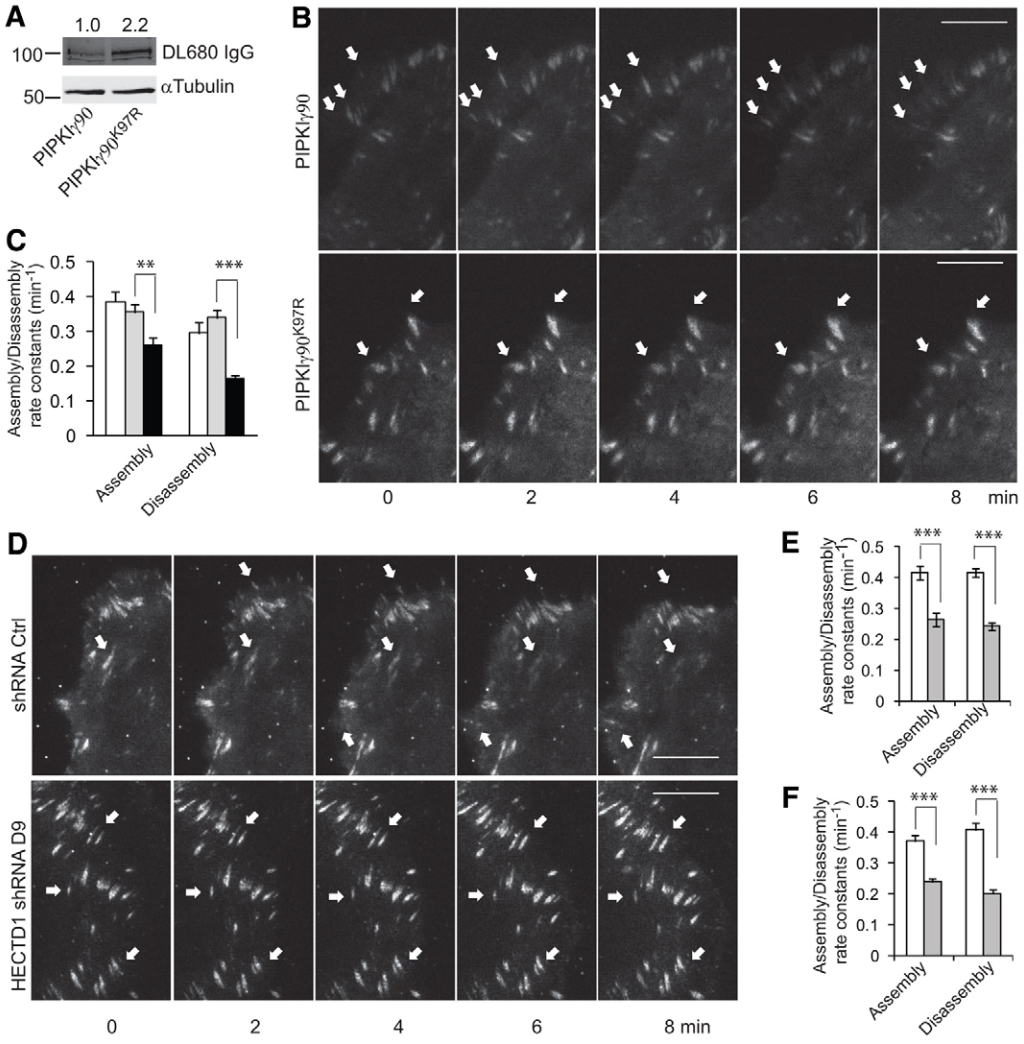

Fig. 3. PIPKIγ90 ubiquitylation by HECTD1 regulates FA assembly and disassembly. (**A**) Expression of ZZ-PIPKIγ90 or ZZ-PIPKIγ90^{K97R} in MDA-MB-231 cells was examined by western blotting. (**B**) MDA-MB-231 cells were infected with lentiviruses that express mDsRed-paxillin and then infected with retroviruses expressing ZZ-PIPKIγ90 or ZZ-PIPKIγ90^{K97R}. The cells were plated on fibronectin and the dynamics of paxillin was analyzed using time-lapse TIRF microscopy. Arrowheads point to dynamic (upper panels) and stable (lower panels) FAs. (**C**) Quantification of the FA assembly and disassembly rate constants in parental MDA-MB-231 cells (white) and cells that stably express ZZ-PIPKIγ90 WT (gray) or ZZ-PIPKIγ90^{K97R} (black). Results are expressed as mean ± s.e.m. of 50 FAs from 10 cells. (**D**) MDA-MB-231 cells that stably express a control (upper panels) or HECTD1 shRNA D9 (lower panels) were infected with retroviruses expressing mDsRed-paxillin. Arrowheads point to dynamic (upper panels) and stable (lower panels) FAs. (**E**) Quantification of the FA assembly and disassembly rate constants in cells that express shRNA control (white) and HECTD1 shRNA (gray). Results are expressed as mean ± s.e.m. of 90 FAs from 20 cells. (**F**) Quantification of the FA assembly and disassembly rate constants in cells that express shRNA control (white) and PIPKIγ shRNA (gray). Results are expressed as mean ± s.e.m. of 50 FAs from 10 cells. $^{**}P<0.01$, $^{***}P<0.001$. Scale bars: 20 μm.

MDA-MB-231 cells are significantly higher than those reported previously in CHO-K1 cells (Huang et al., 2009; Wu et al., 2011), and PIPKIγ90^{K97R} significantly inhibited FA disassembly and slightly reduced FA assembly rate **(**Fig. 3B,C; supplementary material Movies 1, 2**)**. PIPKIγ90 stimulated small FA (<3 μm^2) formation in the centers of the cells (supplementary material Fig. S3A,B). The stimulation of small FA formation by PIPKIγ90 requires its ubiquitylation, because PIPKIγ90^{K97R} was less effective. PIPKIγ90^{K97R}-R accumulated in large FAs (14.1 FAs with area >1 μm^2 per cell, n=8), most of which were localized in the rear of the cells, whereas the WT enzyme formed smaller FAs at the leading edges of the cells (2.8 FAs with area >1 μm^2 per cell, n=13); expression of PIPKIγ90^{K97R}-R also stimulated stress fiber formation (supplementary material Fig. S3C). These results indicate that PIPKIγ90 ubiquitylation is essential for FA disassembly in MDA-MB-231 cells.

To examine whether HECTD1 depletion influences FA dynamics in MDA-MB-231 cells, the cells that stably express DsRed-paxillin were infected with lentiviruses that express a control or HECTD1 shRNA (D9), and FA assembly and disassembly were examined as described above. Depletion of endogenous HECTD1 significantly inhibited both FA assembly and disassembly rates **(**Fig. 3D,E**)**. Depletion of endogenous PIPKIγ90 also suppressed FA disassembly rates and to less extent the assembly rates (Fig. 3F). HECTD1 partially colocalized with talin at the actin arcs immediately behind the

lamellipodium (supplementary material Fig. S3D), where FA in association with actin filaments and myosin (Gupton and Waterman-Storer, 2006; Koestler et al., 2008). These results suggest that dynamic spatial regulation of PIPKIγ90 ubiquitylation by HECTD1 is essential for efficient FA assembly and disassembly.

HECTD1-mediated PIPKIγ90 ubiquitylation is essential for breast cancer cell migration

Since FA dynamics is a key point that regulates cell migration and is also involved in cancer invasion (Webb et al., 2002; Ridley et al., 2003), we set out to examine the role of PIPKIγ90 ubiquitylation in breast cancer cell migration and invasion. To eliminate the interference of endogenous PIPKIγ90, we depleted endogenous PIPKIγ90 and expressed codon-modified WT and ubiquitylation-deficient mutant of PIPKIγ90 to determine whether they restore the function of PIPKIγ90.

MDA-MB-231 cells were infected with lentiviruses that stably express a control or PIPKIγ90 shRNA (supplementary material Fig. S4A). The cells were plated on glass-bottomed dishes coated with 5 μg/ml fibronectin, and the migration was determined by time-lapse cell migration assays. Depletion of endogenous PIPKIγ90 significantly reduced the velocity and directionality of cell migration, and strongly inhibited the net distance of cell migration (supplementary material Fig. S4B,C), indicating that PIPKIγ90 modulates cell migration by controlling the velocity and directionality of migration.

To test whether PIPKIγ90 ubiquitylation regulates the migration of breast cancer cells, MDA-MB-231 cells that express PIPKIγ90 shRNA were infected with retroviruses expressing ZZ-PIPKIγ90-R or ZZ-PIPKIγ90^{K97R}-R, respectively, and cell migration was determined by time-lapse cell migration assays as described above. The expression of WT PIPKIγ90-R and PIPKIγ90^{K97R}-R was much higher than that of endogenous PIPKIγ (Fig. 4A). While WT PIPKIγ90-R restored the migration of PIPKIγ-depleted cells, PIPKIγ90^{K97R}-R was unable to do that (Fig. 4B,C; supplementary material Movies 3–5). PIPKIγ90^{K97R}-R impaired cell migration mainly through inhibiting the persistence of the lamellipodium protrusions (Fig. 4D), consequently suppressing the directionality (Fig. 4B). This conclusion is further supported by that expression of HECTD1 shRNA also suppressed the directionality of cell migration (Fig. 5A,B). Both PIPKIγ90^{K97R} and HECTD1 shRNA inhibited the directionality of migration, suggesting that PIPKIγ90 ubiquitylation regulates cell migration by mainly controlling the directionality.

PIPKIγ90 ubiquitylation by HECTD1 regulates cancer cell invasion and metastasis

To examine the role of PIPKIγ90 in breast cancer cell invasion, MDA-MB-231 cells were infected with lentiviruses that express PIPKIγ90 shRNA or an empty vector. The invasion of these cells was measured by examining the functional capacities of the cells penetrating through transwell filters coated with 0.35 mg/ml Matrigel. Depletion of endogenous PIPKIγ90 inhibited the invasion of MDA-MB-231 cells (Fig. 6A). To examine the role of PIPKIγ90 ubiquitylation in breast cancer cell invasion, PIPKIγ90-depleted cells were infected with retroviruses that express WT PIPKIγ90-R and PIPKIγ90^{K97R}-R, respectively. The invasion of these cells was compared to that of the PIPKIγ90-depleted cells and cells infected with the shRNA control. Re-expression of codon-modified WT PIPKIγ90-R in PIPKIγ90-depleted cells restored the invasion of the PIPKIγ90-depleted

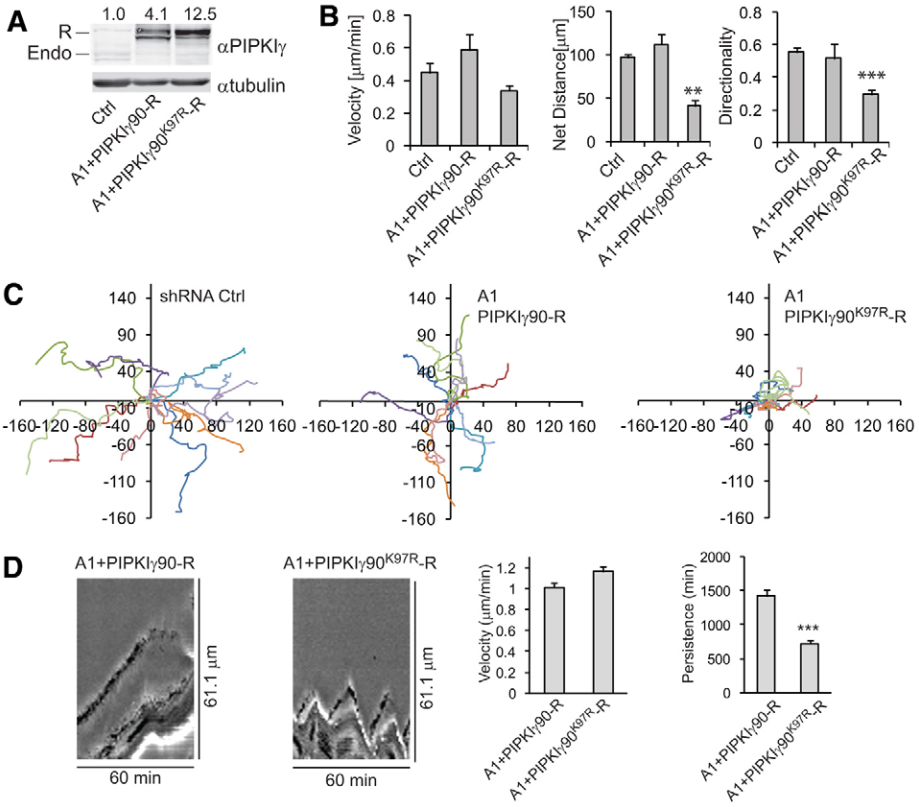

Fig. 4. PIPKIγ90 ubiquitylation regulates protrusion persistence and directional migration. (**A**) Expression of ZZ-PIPKIγ90-R or ZZ-PIPKIγ90^{K97R}-R in MDA-MB-231 cells compared with endogenous PIPKIγ. (**B**) Velocity, net distance, total path and directionality of the cells expressing a control shRNA (Ctrl) and the PIPKIγ-depleted cells stably expressing ZZ-PIPKIγ90-R or ZZ-PIPKIγ90^{K97R}-R. The data are expressed as mean ± s.e.m. of more than 53 cells from three independent experiments; $^{**}P<0.01$ and $^{***}P<0.001$ compared with control cells. (**C**) Migration tracks of ten MDA-MB-231 cells that express a control shRNA and ten PIPKIγ-depleted MDA-MB-231 cells that stably express ZZ-PIPKIγ90-R or ZZ-PIPKIγ90^{K97R}-R. (**D**) PIPKIγ90 ubiquitylation regulates the persistence of lamellipodium protrusions. Left, kymograph of lamellipodial dynamics. Right, quantitative analysis of lamellipodial velocity and persistence. Data are mean ± s.e.m. Persistence, $n=90$, $^{***}P<0.001$; velocity, $n=79$, $P>0.05$.

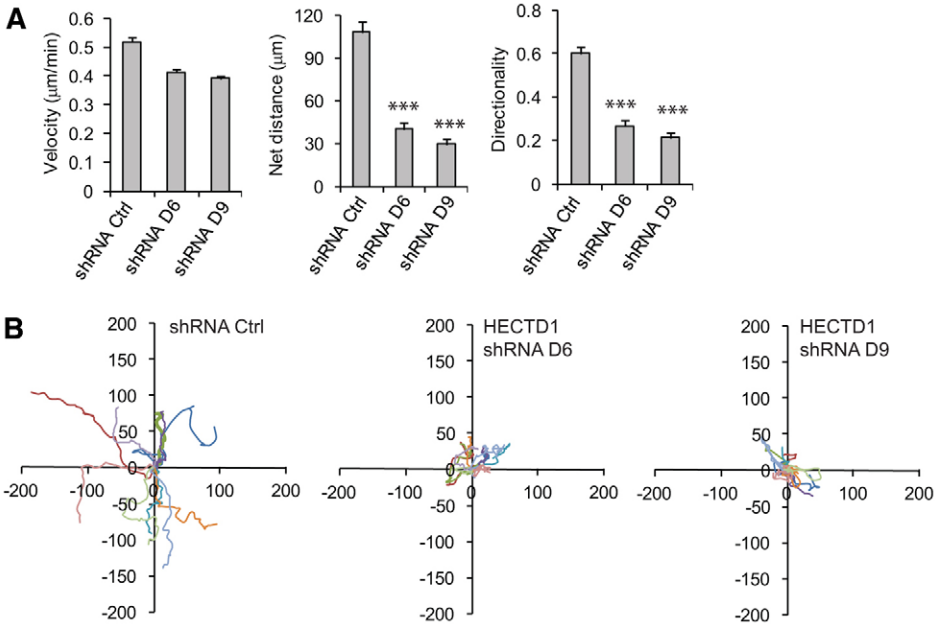

Fig. 5. HECTD1 is required for efficient directional migration. (**A**) Velocity, net distance, total path and directionality of the cells stably expressing shRNA control or HECTD1 shRNA D6 or D9. The data are expressed as mean ± s.e.m. of more than 50 cells from at least three independent experiments; ***$P<0.001$ compared with control cells. (**B**) Migration tracks of ten MDA-MB-231 cells that stably express a shRNA control, HECTD1 shRNA D6 or D9 transposed to a common origin.

cells, whereas that of the PIPKIγ90^{K97R} counterpart did not (Fig. 6B,C). Similar results were observed in MDA-MB-468 and MDA-MB-157 cells (Fig. 6D,E). In addition, depletion of endogenous HECTD1 also inhibited the invasion of MDA-MB-231 cells (Fig. 6F). These results indicate that HECTD1-mediated ubiquitylation of PIPKIγ90 is essential for breast cancer cell invasion.

To delineate whether there is any correlation between PIPKIγ ubiquitylation and cancer cell invasion, highly invasive (invade in 8 hours) and non-invasive (do not invade in 16 hours) MDA-MB-231 cells were recovered from transwell invasion assays and grown in normal medium. The cells were treated with DMSO or bortezomib plus carfilzomib and steady-state levels of PIPKIγ were examined. While treatment with proteasome inhibitors resulted in a significant increase in the steady-state levels of HECTD1 and PIPKIγ in highly invasive cells, HECTD1 and PIPKIγ levels were not increased in the non-invasive cells (Fig. 6G). Because the autoubiquitylation is essential for the activity of HECT domain E3 ubiquityl ligases (Gao et al., 2004; Lu et al., 2008), the high basal HECTD1 level in the non-invasive cells is equivalent to low E3 ligase activity, which correlates with the low ubiquitylation of PIPKIγ in these cells. In addition, the higher PIPKIγ ubiquitylation in MDA-MB-231 cells, as compared to that in MDA-MB-468 and MDA-MB-157 cells (Fig. 1A), correlated with more aggressive invasion of MDA-MB-231 cells. These results suggest that PIPKIγ ubiquitylation regulates invasive capacity of cancer cells.

Since PIPKIγ90 ubiquitylation regulates cancer cell migration and invasion, key steps in cancer metastasis, we examined whether PIPKIγ90 ubiquitylation regulates the metastasis of breast cancer cells by mouse tail vein metastasis assays. MDA-MB-231 cells infected with a control shRNA and PIPKIγ-depleted cells that re-expressed WT ZZ-PIPKIγ90-R or ZZ-PIPKIγ90^{K97R}-R were injected into the tail vein of female ICR-SCID mice. After 6 weeks, mice were euthanized and lungs were removed and photographed. Tumor nodules present on the surface of the lungs were examined microscopically. The lungs from the mice injected with the cells expressing PIPKIγ90-R were similar to those injected with the cells infected with the control shRNA, but had dramatically more tumor nodules than those injected with the cells expressing PIPKIγ90^{K97R}-R (Fig. 7A,B). Also, hematoxylin and eosin (H&E) staining showed that the lung sections from the mice injected with cells expressing PIPKIγ90-R demonstrated numerous tumor nodules, whereas those from mice injected with cells expressing PIPKIγ90^{K97R}-R had few or no tumor nodules (Fig. 7C). These results indicate that PIPKIγ90 ubiquitylation is essential for the experimental metastasis of MDA-MB-231 cells.

PIPKIγ90-talin interaction is responsible for the effect of PIPKIγ90^{K97R}

To dissect the molecular mechanisms whereby PIPKIγ90 ubiquitylation regulate FA dynamics, cell migration and invasion, we examined whether the interaction of PIPKIγ90 with talin mediates the effect of PIPKIγ90^{K97R}. We substituted tryptophan 647 (W647), a key residue responsible for PIPKIγ90 binding to talin, with Phe and ZZ-PIPKIγ90^{K97R}, ZZ-PIPKIγ90^{W647F} and ZZ-PIPKIγ90^{K97R,W647F} were stably expressed in PIPKIγ-depleted MDA-MB-231 cells by retrovirus infection. The ZZ-tagged proteins were precipitated with IgG–Sepharose, and associated talin was detected using an anti-talin antibody. PIPKIγ90^{K97R} co-precipitated with talin, whereas mutation at W647 almost abolished the co-precipitation (Fig. 8A). Also, PIPKIγ90^{K97R} localized to FA, while mutation at W647 blocked its distribution at FA (supplementary material Fig. S5). To examine whether the interaction of PIPKIγ90 with talin mediates the effect of PIPKIγ90^{K97R} on FA assembly and disassembly, the PIPKIγ-depleted MDA-MB-231 cells that stably express ZZ-PIPKIγ90^{K97R} and ZZ-PIPKIγ90^{K97R,W647F}, respectively, and parental MDA-MB-231 cells carrying an empty pBabe vector were infected with retroviruses that express DsRed-paxillin. FA dynamics were examined by monitoring DsRed–paxillin using time-lapse TIRF microscopy. PIPKIγ90^{K97R} significantly inhibited FA assembly and disassembly rates, but PIPKIγ90^{K97R,W647F} did not (Fig. 8B).

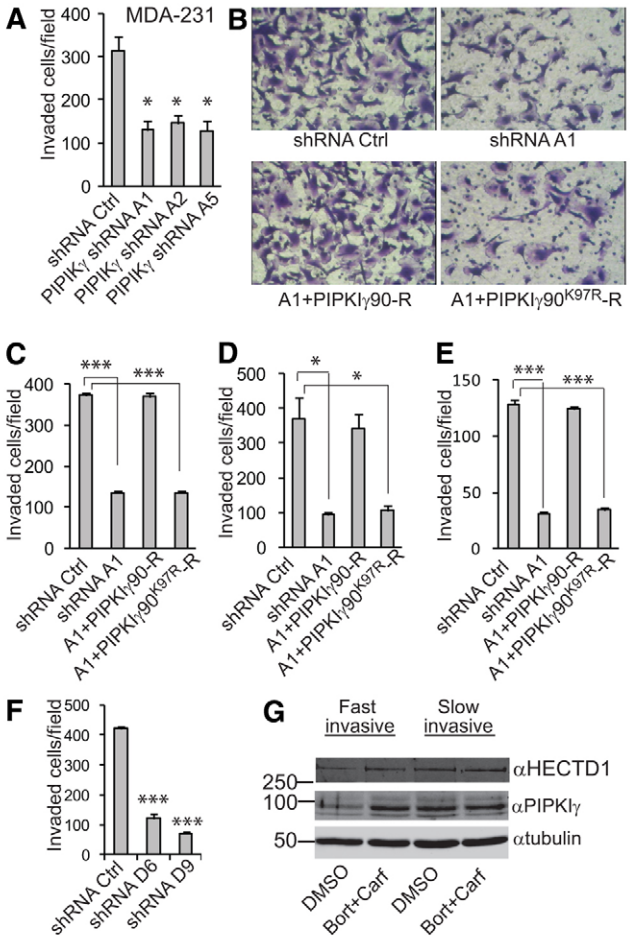

Fig. 6. PIPKIγ90 ubiquitylation by HECTD1 is required for breast cancer cell invasion. (**A**) Depletion of endogenous PIPKIγ inhibited the invasion of MDA-MB-231 cells. The cells were infected with pLKO1 lentiviruses that express shRNA control or PIPKIγ90 shRNAs and then selected with puromycin; $n=5$. (**B**) PIPKIγ90 restored the invasive capacity of PIPKIγ-depleted MDA-MB-231 cells, but PIPKIγ90^{K97R} did not. The PIPKIγ-depleted MDA-MB-231 cells were infected with retroviruses that express ZZ-PIPKIγ90-R or ZZ-PIPKIγ90^{K97R}-R and then selected with neomycin. The PIPKIγ-depleted cells and cells expressing shRNA control were used as controls. (**C**) Quantification of experiment B. (**D**) PIPKIγ90 restored the invasive capacity of PIPKIγ-depleted MDA-MB-468 cells, but PIPKIγ90^{K97R} did not; $n=5$. (**E**) Quantification of the invasion of PIPKIγ-depleted MDA-MB-157cells stably expressing ZZ-PIPKI-R or ZZ-PIPKIγ90^{K97R}-R, using PIPKIγ-depleted cells and cells expressing shRNA control as controls; $n=5$. (**F**) Depletion of endogenous HECTD1 inhibited the invasion of MDA-MB-231 cells. The cells were infected with pLKO1 lentiviruses expressing shRNA control or HECTD1 shRNA and then selected with puromycin. $n=3$. (**G**) Steady-state levels of PIPKIγ and HECTD1 were determined by western blotting in fast invasive or slow invasive MDA-MB-231 cells ($n=5$) that were treated with DMSO or bortezomib plus carfilzomib (1 μM each). Data are presented as mean ± s.e.m. $^*P<0.05$, $^{***}P<0.001$ compared with control cells.

The migration of the PIPKIγ-depleted MDA-MB-231 cells that stably express ZZ-PIPKIγ90^{K97R} and ZZ-PIPKIγ90^{K97R,W647F}, respectively was also examined, using parental MDA-MB-231 cells carrying an empty pBabe vector as a control. Mutation at W647 partially rescued the suppression of PIPKIγ90^{K97R} on cell migration (Fig. 8C,D). To examine whether the interaction of

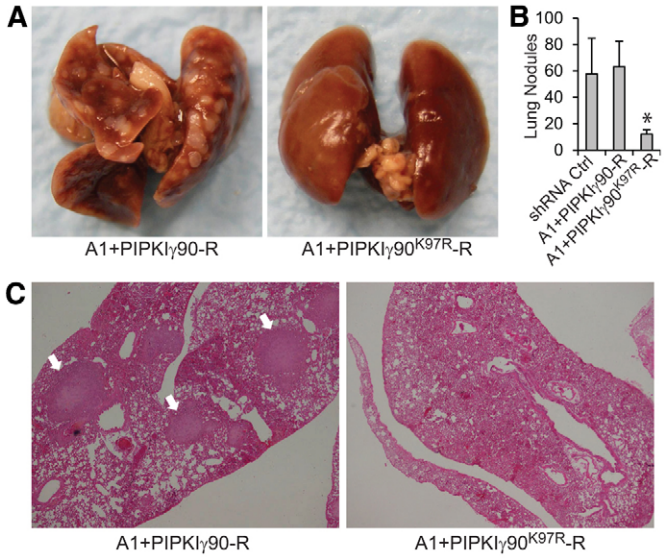

Fig. 7. PIPKIγ90 ubiquitylation by HECTD1 is required for breast cancer cell metastasis. (**A**) PIPKIγ-depleted MDA-MB-231 cells expressing ZZ-PIPKIγ90-R or ZZ-PIPKIγ90^{K97R}-R were injected into the tail veins of ICR-SCID mice. After 6 weeks, lungs were excised. Representative lungs are shown from mice implanted with PIPKIγ-depleted cells stably expressing PIPKIγ90-R or PIPKIγ90^{K97R}-R. (**B**) The number of tumor nodules on the lung surface was examined under a dissection microscope and plotted; $^*P<0.05$. (**C**) Hematoxylin and eosin staining (40×) of paraffin-embedded sections of lung specimens from nude mice implanted with PIPKIγ-depleted cells stably expressing PIPKIγ90-R or PIPKIγ90^{K97R}-R. Arrows point to tumor nodules.

PIPKIγ90 with talin mediates the effect of PIPKIγ90^{K97R} on breast cancer cell invasion, we expressed ZZ-PIPKIγ90^{K97R}, ZZ-PIPKIγ90^{W647F} and ZZ-PIPKIγ90^{K97R,W647F} in PIPKIγ-depleted MDA-MB-231 cells and tested the Matrigel invasive capacity of these cells, using parental MDA-MB-231 cells carrying an empty pBabe vector as control. Both PIPKIγ90^{K97R,W647F} and PIPKIγ90^{W647F} partially rescued the invasive capacity suppressed by PIPKIγ90 knockdown, but PIPKIγ90^{K97R} did not (Fig. 8E). All these results suggest that constant PIPKIγ90-talin interaction is partially responsible for the effect of PIPKIγ90^{K97R}, and that PIPKIγ90 ubiquitylation by HECTD1 provides a mechanism to remove PIPKIγ90 spatially and temporarily, thus regulating FA dynamics, cell migration and invasion.

Discussion

PIPKIγ90 is a key enzyme that catalyzes the phosphorylation of PIP to generate PIP_2, which regulates a variety of physiological and pathological processes, including FA dynamics, cell migration and cancer metastasis (Ling et al., 2006; van Rheenen et al., 2007; Qin et al., 2009; Sosa et al., 2010). PIPKIγ90 interacts with talin and generated on-site PIP_2, which can, in turn promote talin binding to the β-integrin tail by blocking the self-inhibition of talin (head-tail interaction) (Goksoy et al., 2008; Goult et al., 2009). PIP_2 can also stimulate integrin clustering (Saltel et al., 2009). However, PIPKIγ90 shares the same binding site on talin with the β-integrin tail (Barsukov et al., 2003; de Pereda et al., 2005). Thus the interaction of talin with PIPKIγ can hinder its binding to the β-integrin tail (Calderwood et al., 2004). Our results show that

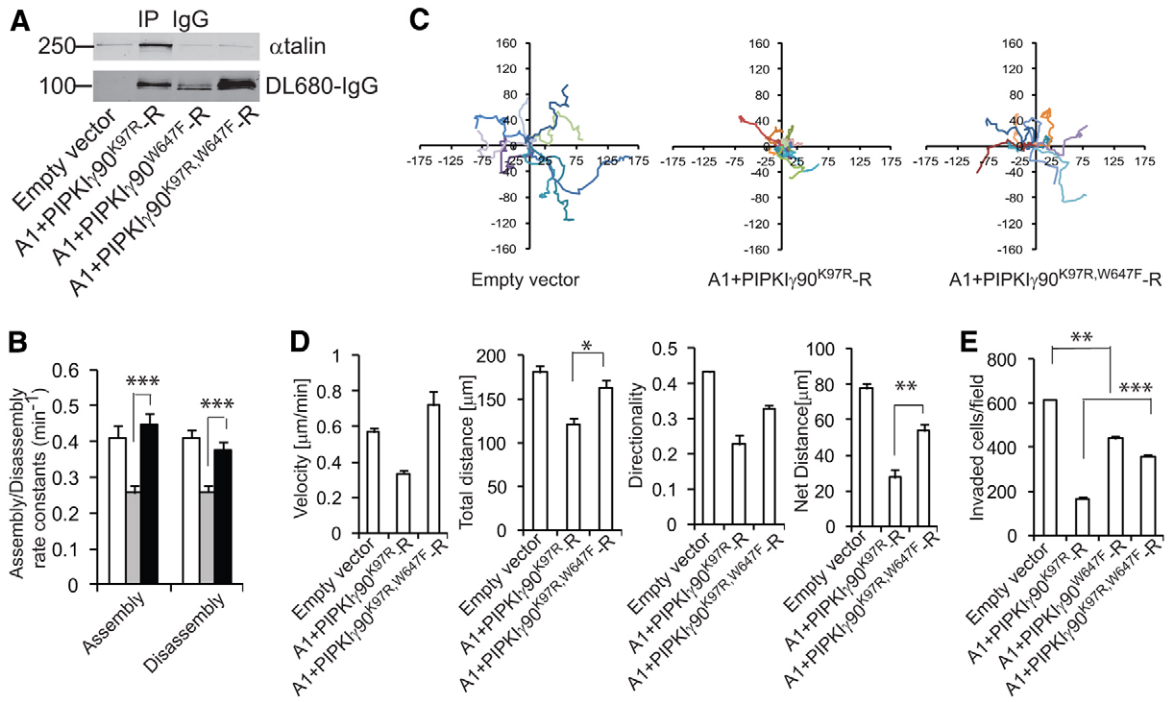

Fig. 8. PIPKIγ90-talin interaction mediates the inhibitory effect of PIPKIγ90^{K97R}. (**A**) Co-immunoprecipitation of talin with ZZ-PIPKIγ90^{K97R}-R, ZZ-PIPKIγ90^{W647F}-R and ZZ-PIPKIγ90^{K97R,W647F}-R that were expressed in PIPKIγ-depleted MDA-MB-231 cells. (**B**) Quantification of the FA assembly and disassembly rate constants in PIPKIγ-depleted MDA-MB-231 cells stably expressing ZZ-PIPKIγ90^{K97R}-R (gray), or ZZ-PIPKIγ90^{K97R,W647F}-R (black) and in parental MDA-MB-231 cells carrying an empty pBabe vector (white). Results are expressed as mean ± s.e.m. of 50 FAs from 10 cells. (**C**) Migration tracks of ten MDA-MB-231 cells carrying an empty pBabe vector and ten PIPKIγ-depleted MDA-MB-231 cells stably expressing ZZ- PIPKIγ90^{K97R}-R or ZZ-PIPKIγ90^{K97R,W647F}-R. (**D**) Velocity, net distance, total path and directionality of the cells carrying an empty pBabe vector and the PIPKIγ-depleted cells stably expressing ZZ-PIPKIγ90^{K97R}-R or ZZ-PIPKIγ90^{K97R,W647F}-R. The data are expressed as mean ± s.e.m. of more than 60 cells from three independent experiments. (**E**) Mutation at W647 partially reversed the inhibition of PIPKIγ90^{K97R} on the invasion of MDA-MB-231 cells. The invasive capacity of PIPKIγ-depleted cells expressing ZZ-PIPKIγ90^{K97R}-R, ZZ-PIPKIγ90^{W647F}-R and ZZ-PIPKIγ90^{K97R,W647F}-R was determined by Matrigel assays, using parental cells carrying an empty pBabe vector as a control (n=5). *P<0.05, **P<0.01, ***P<0.001.

PIPKIγ90 is ubiquitylated by HECTD1 at K97, resulting in its degradation, thus regulating FA dynamics. Therefore, we propose that after generating PIP_2 on-site for FA formation, PIPKIγ90 is ubiquitylated by HECTD1 and degraded consequently releasing its inhibition on talin–β-integrin-tail interaction, thus promoting integrin activation and FA formation. Our study elucidates how PIPKIγ90 binds talin to provide PIP_2 on-site but does not impair the talin–β-integrin tail interaction. Importantly, our results provide novel insights into the molecular mechanisms which regulate FA dynamics and cell migration.

We demonstrated that PIPKIγ90 was ubiquitylated by Smurf1 in CHO-K1 cells (supplementary material Fig. S1B). We previously reported that the talin head was also ubiquitylated by Smurf1 (Huang et al., 2009). However, depletion of Smurf1 did not affect endogenous PIPKIγ levels in MDA-MB-231 breast cancer cells (supplementary material Fig. S1C). HECTD1 is an E3 ubiquitin ligase homologous to Smurf1. It has been shown that HECTD1 regulates cell migration and neural tube closure (Zohn et al., 2007; Sarkar and Zohn, 2012). We showed here that HECTD1 ubiquitylated PIPKIγ90 at K97 and that HECTD1 knockdown resulted in an increase in endogenous PIPKIγ90 levels (Fig. 1C,D,G), indicating that HECTD1 is responsible for the ubiquitylation of PIPKIγ90 in these cancer cells. PIPKIγ90 ubiquitylation resulted in its degradation, which was prevented by proteasome inhibitors. Expression of PIPKIγ90^{K97R}, an ubiquitylation-resistant mutant, enhanced PIP_2 and PIP_3 production in MDA-MB-231 cells (Fig. 2A). These results suggest that PIPKIγ90 ubiquitylation represents a new regulatory mechanism for the phosphoinositide signaling pathways.

$PI(4,5)P_2$, the direct product of PIPKIγ90, regulates the functions of many cytoskeletal and FA proteins as well as serving as the precursors of other signaling molecules. $PI(4,5)P_2$ interacts with vinculin to unmask the talin-binding sites on vinculin (Gilmore and Burridge, 1996); it also binds talin thus suppressing the head-tail interaction of talin and stabilizing talin-integrin interactions (Martel et al., 2001; Saltel et al., 2009). PIPKIγ90 is thought to be the enzyme that generates $PI(4,5)P_2$ spatially and temporally for FA formation during cell migration (Ling et al., 2002; Ling et al., 2006). PIPKIγ90 has been shown to be required for FA formation during EGF-stimulated cell migration (Sun et al., 2007), whereas it has also been reported that expression of PIPKIγ90 caused cell rounding and FA disassembly (Di Paolo et al., 2002).

Here, we show that depletion of HECTD1 significantly suppressed both FA assembly and disassembly rates (Fig. 3D,E) and that expression of PIPKIγ90^{K97R}, an ubiquitylation-resistant mutant, inhibited both FA assembly and disassembly rates in MDA-MB-231 cells (Fig. 3B,C). On the other hand, the mutation at W647 abolished the suppression of PIPKIγ90^{K97R} on FA assembly and disassembly rates (Fig. 8B). PIPKIγ^{K97R} is resistant

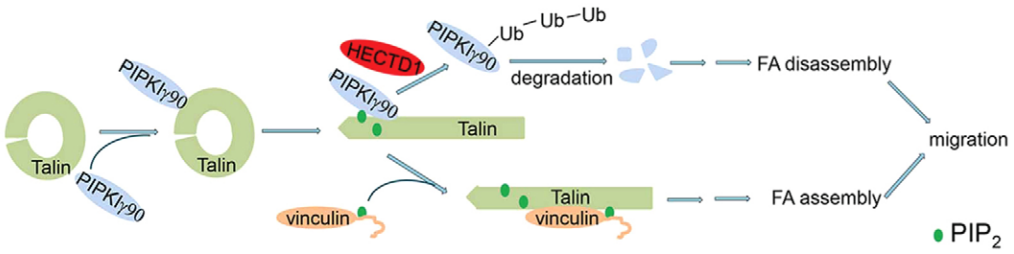

Fig. 9. Hypothetical model for the role of HECTD1-mediated PIPKIγ90 ubiquitylation in regulating FA assembly and disassembly and cell migration.

to degradation and is able to bind talin; PIPKIγ90^{K97R,W647F} is also resistant to degradation but has a reduced binding capacity for talin. Based on these results, we propose a hypothetical model to illustrate the role of PIPKIγ90 in regulating FA dynamics (Fig. 9). PIPKIγ90 is recruited by talin to produce on-site PIP_2, which in turn interacts with talin and vinculin thus unmasking the head-tail interaction of talin and vinculin (Gilmore and Burridge, 1996; Goksoy et al., 2008; Goult et al., 2009). The binding of the β-integrin tail to talin is also enhanced by PIP_2, resulting in integrin activation and FA assembly (Martel et al., 2001; Saltel et al., 2009; Legate et al., 2011). PIPKIγ90^{K97R,W647F} is deficient in talin-binding but did not significantly inhibit FA assembly and disassembly, probably because its higher expression (ubiquitylation-resistant) compensates its deficiency in talin binding. On the other hand, PIPKIγ90 is ubiquitylated by HECTD1 and subsequently degraded, consequently reducing PIP_2 production and weakening the β-integrin–talin interaction. Proteolysis of talin by calpain and Smurf1-regulated subsequent ubiquitylation of the talin head as well as myosin-mediated contraction could cause FA disassembly (Franco et al., 2004; Webb et al., 2004; Huang et al., 2009).

Several lines of evidence implicate a role of PIPKIγ90 ubiquitylation in focal adhesion assembly. It has been reported that overexpression of PIPKIγ90 suppresses integrin activation (Calderwood et al., 2004) and that PIPKIγ90 and the β-integrin tail compete for the same site on talin (Barsukov et al., 2003; de Pereda et al., 2005). Also, phosphorylation of PIPKIγ90 by Src promotes its interaction with talin, inhibiting the talin–β-integrin interaction (Ling et al., 2003). Furthermore, either expression of ubiquitylation-resistent PIPKIγ90^{K97R} or knockdown of HECTD1 inhibit focal adhesion assembly (Fig. 3). In addition, PIPKIγ90^{K97R} is less effective than the WT in promoting small FA formation (supplementary material Fig. S3A,B). These data support that PIPKIγ90 ubiquitylation and degradation might facilitate the talin-integrin interaction. However, a recent paper shows that talin-PIPKIγ90-β1 integrin exist as a complex in migrating cells (Thapa et al., 2012). Because talin can form anti-parallel homodimer and has two distinct β-integrin-binding sites, it remains to be determined whether and how PIPKIγ90 ubiquitylation regulates talin–β-integrin interaction.

It has been reported that PIPKIγ90 is required for the migration and invasion of MDA-MB-231 human breast cancer cells and HeLa human cervical cancer cells (Sun et al., 2007; Sun et al., 2010). Consistent with these findings, our results show that depletion of PIPKIγ90 inhibited the migration and invasion of several breast cancer cell lines (Fig. 6A; supplementary material Fig. S4). Also, depletion of HECTD1 inhibited the migration and invasion of MDA-MB-231 cells (Fig. 5; Fig. 6F). Furthermore, re-expression of codon-modified PIPKIγ90-R in PIPKIγ-depleted cells restored the cell migration and invasion to that of the control cells, whereas that of PIPKIγ90^{K97R}-R was unable to do so (Fig. 4B,C; Fig. 6B–E). Mutation at W647 partially rescued the inhibition of PIPKIγ90^{K97R} on cell migration (Fig. 8C,D). Interestingly, re-expression of PIPKIγ90^{K97R,W647F}-R, a mutant defective in focal adhesion targeting and ubiquitylation, restored the cell invasion to the similar level rescued by re-expressing PIPKIγ90^{W647F}-R, pointing to a role of PIP_2 synthesis in cell migration and invasion (Fig. 8E). The invasion was inhibited only when the focal adhesion targeted PIPKIγ90 is resistant to ubiquitylation and focal adhesions persist. Since FA turnover also occurs with 3-dimensional cell matrix (Deakin and Turner, 2011), and FA dynamics has been well documented in regulating cell migration and cancer invasion (Webb et al., 2002; Le et al., 2010; Deakin and Turner, 2011), HECTD1-mediated PIPKIγ90 ubiquitylation may regulate cell migration and invasion by modulating FA dynamics.

Finally, we demonstrate that PIPKIγ90 ubiquitylation is essential for the experimental metastasis of MDA-MB-231 cells (Fig. 7A–C). Hence, our findings in our current study as well as those of others (Miyazaki et al., 2003; Deakin and Turner, 2011) clearly indicate that pathways regulating FAs control cancer metastasis.

In summary, PIPKIγ90 ubiquitylation by HECTD1 and consequent degradation modulate the on-site production of PIP_2, thus regulating focal adhesion dynamics and cell migration. The study provides new insights into the molecular mechanisms regulating cell adhesion and migration.

Materials and Methods

Reagents

IgG-Agarose, pZZ-PIPKIγ90 and pAvi-PIPKIγ90 were described previously (Huang and Jacobson, 2010). Anti-paxillin antibody (clone 5H11) was from Millipore. Anti-PIPKIγ polyclonal antibody was from Epitomics. Anti-ubiquitin antibody was from Cell Signaling Technology (Danvers, MA). Anti-talin, anti-VSVG and anti-tubulin antibody and pLKO1 lentivirus shRNAs that respectively target PIPKIγ90, HECTD1, Smurf1 and Smurf2 were from Sigma; PIPKIγ90 shRNA clones are TRCN0000037668 (A1), TRCN0000037664 (A2) and TRCN0000195424 (A5); HECTD1 shRNA clones are TRCN0000004084 (D6) and TRCN0000004087 (D9); Smurf1 and Smurf2 shRNA clones are TRCN0000003472 and TRCN0000003477, respectively; DyLight 549 conjugated goat anti-mouse IgG (H^+L) was from Thermo Scientific; Fibronectin and recombinant human EGF were from Akron Biotech; Growth factor reduced Matrigel was from BD Bioscience; Pfu Ultra was from Agilent Technologies; cDNA clones Lifeseq3465723 and 3648730 were purchased from Open Biosystems; Endura^{TM} competent cells were from Lucigen; Safectine RU50 transfection kit was purchased from Syd Labs (Malden, MA) and anti-HECTD1 rabbit polyclonal antibody was custom made by Syd Labs; DNA primers were synthesized by Integrated DNA Technologies.

Plasmid construction

The full-length pEGFP-HECTD1 was subcloned by following steps: (1) DNA fragments encoding residues 1841–2610 of human HECTD1 were amplified by pfu Ultra-based PCR using Lifeseq3465723 cDNA clone as template and 5′-TTCAGGTCGACCATCTTTTACTATGTACAAAAATTGCTTCAATTGTCC-3′, 5′-ATTATATCTAGATCAATTGAGATGAAAGCCTTTCTCCATTGTAGCAGC-3′ and subcloned into pEGFP-paxillin β (Huang et al., 2003) (as a vector) via Sal1/Xba1 sites; (2) fragments encoding residues 1421–1842 of HECTD1 were amplified

using Lifeseq3648730 as template and 5′-GAAGTAGGATCCTCTTCCAGTG-CAAGCACCAGCACC-3′, 5′-AAGATGGTCGACCTGAAATTGGTGAGTGGT-AATTCAACTTC-3′ and subcloned into the resulted plasmid in step 1 via BamH1/Sal1 sites; (3) fragments encoding residues 786–1422 with several silent mutations (synthesized by Invitrogen) were subcloned into the resulted plasmid in step 2 via XmaI/BamH1; and (4) fragments encode residues 1–787 with a number of silent mutations (by Invitrogen) were subcloned into the resulted plasmid in step 3 via *Bgl*II/Xma1 sites and transformed Endura^{TM} competent cells. The plasmid pZZ-PIPKIγ90^{K97R} and pAvi-PIPKIγ90^{K97R} was generated by pfu Ultra-based PCR using pZZ-PIPKIγ90 and pAvi-PIPKIγ90 as templates, respectively, and 5′-CA-CCTGAGCTCCAGACCCGAACGC-3′, 5′-GCGTTCGGGTCTGGAGCTCAGG-TG-3′ as primers. The rescue plasmid pZZ-PIPKIγ90-R and pZZ-PIPKIγ90^{K97R}-R were created by PCR using pZZ-PIPKIγ90 and pZZ-PIPKIγ90^{K97R} as templates and sequentially 5′-TTCATGAGCAATACCGTCTTTCGG-3′, 5′-CCGAAAGACGG-TATTGCTCATGAA-3′ and 5′-GTCTTTCGGAAAAATTCCTCCCTG-3′, 5′-CA-GGGAGGAATTTTTCCGAAAGAC-3′ as primers. The pBabe-ZZ-PIPKIγ90-R and pBabe-ZZ-PIPKIγ90^{K97R}-R were made by sequentially digesting pZZ-PIPKIγ90-R and pZZ-PIPKIγ90^{K97R}-R with Age1, blunting with Klenow and digesting with Sal1. The smaller fragments were subcloned into pBabe-neo vector that had been treated with BamH1, Klenow and Sal1. pDsRed-paxillin was generated by PCR amplifying DsRed using pDsRed-monomer-N1 (Clontech) as template and 5′-GGATCCACCGGTCGCCACCATG-3′, 5′-AAAAAACTCGA-GGCTGGGAGCCGGAGTGGCGGGC-3′ primers. The PCR products were digested with Age1 and Xho1 and inserted into pEGFP-paxillin (Huang and Jacobson, 2010) cut with the same enzymes. pLL3.7-DsRed-paxillin was constructed by treating pDsRed-paxillin sequentially with Sal1, Klenow and Age1 and inserting into the pLL3.7 lentiviral vector that was treated with EcoR1, Klenow and Age1. pAvi-Ubiquitin was created by digesting pcDNA-HA-ubiquitin with BamH1, treating with Klenow and cleaving with Xho1. The smaller fragments were subcloned into pAvi vector that was treated sequentially with Xho1, Klenow and Sal1. The resulted plasmid was digested with *Bgl*II, treated with Klenow and ligated. All plasmids were sequenced by Eurofins MWG Operon (Huntsville, AL).

Cell culture and transfection

CHO-K1 Chinese hamster ovary cells, MDA-MB-231, MDA-MB-468 and MDA-MB-157 human breast cancer cells and 293T human embryonic kidney cells were from the American Type Culture Collection and were maintained in DMEM medium (Mediatech, Inc.) containing 10% fetal bovine serum (FBS), penicillin (100 U/ml) and streptomycin (100 μg/ml). CHO-K1 and 293T cells were transfected with Safectine RU50 according to the manufacturer's protocol.

Preparation of viruses and cell infection

The 293T cells were transfected with pBabe retroviral, pLL3.7 or pLKO1 lentiviral system using Safectine RU50 transfection reagent according to the manufacturer's protocol. The virus particles were applied to overnight cultures of breast cancer cells for infection. Cells that stably express pLKO1 lentiviral shRNAs were obtained by selecting the infected cells with 1 μg/ml puromycin, and cells that were infected with pBabe retroviruses were stabilized by growing infected cells in the presence of 0.7 mg/ml neomycin for 10 days. Cells that stably express DsRed-paxillin were established by infecting the cells with pLL3.7-DsRed-paxillin lentiviruses and sorting DsRed positive cells by flow cytometry.

Real-time quantitative PCR

Total RNA was extracted from cells with PureLink RNA kit (Ambion). cDNA was synthesized with SuperScript First Strand Synthesis kit (Invitrogen) from 0.5 to 1.0 μg RNA samples according to the manufacturer's instructions. Quantitative reverse transcriptase PCR (RT-PCR) reactions were carried out using SYBR Green PCR master mix reagents on an ABI Onestep Plus Real-Time PCR System (Applied Biosystems). The relative quantification of gene expression for each sample was analyzed by the ΔC_t method. The following primers were used to amplify PIPK1γ90: 5′-CGTCTGGACAGGATGGCAGGC-3′ and 5′-TGTGT-CGCTCTCGCCGTCGGA-3′; 18S rRNA: 5′-ACCTGGTTGATCCTGCCAGT-3′ and 5′-CTGACCGGGTTGGTTTTGAT-3.

Ubiquitylation assays

ZZ-PIPKIγ90 (or ZZ-PIPKIγ90^{K97R}) and Avi-ubiquitin were co-transfected with an ubiquitin ligase or an empty vector into CHO-K1 cells stably expressing EGFP-BirA (Huang and Jacobson, 2010). At 24 hours post-transfection, cells were incubated with 500 μM of biotin and 1 μM of bortezomib and 1 μM of carfilzomib for 6 hours, and then scraped in PBS. The cells were spinned down, lysed with 150 μl of 1× SDS sample buffer (without 2-mercaptoethanol) containing protease inhibitor cocktail and Bortezomib/Carfilzomib and boiled immediately. The lysates were cleared, diluted to 1 ml and incubated with rabbit IgG-Sepharose beads at 4℃ for 2 hours to precipitate ZZ tagged PIPKIγ90 (or PIPKIγ90^{K97R}) domain fusion protein. The beads were washed, analyzed by SDS-PAGE and western blot as above. The ubiquitylation of the ZZ domain fusion protein was detected with Dylight 680-Streptavidin, while the expression of the ZZ domain fusion protein was probed with Dylight 680-rabbit IgG.

In vitro PIPKIγ90 activity assays

CHO-K1 cells were transfected with pZZ-PIPKIγ90 or pZZ-PIPKIγ90^{K97R}. At 24 hours post-transfection, the cells were harvested in a lysis buffer (50 mM Tris-HCl, pH 8.1, 140 mM NaCl, 50 mM NaF, 1% Triton X-100, 10 mM 2-mercaptoethanol, 0.5 mM AEBSF, 10 μg/ml aprotinin, 10 μg/ml leupeptin, 5 μg/ml E-64, 5 μg/ml pepstatin, 5 μg/ml bebstatin). Cell lysates were cleared by centrifugation and pZZ-PIPKIγ90 and pZZ-PIPKIγ90^{K97R} in supernatants were immunoprecipitated using IgG-Agarose beads. The beads were washed three times with lysis buffer and washed once with a kinase buffer (50 mM Tris-HCl, pH 7.5, 5 mM $MgCl_2$, 25 mM KCl, 0.5 mM EGTA and 0.5 mM ATP). The beads were incubated with 100 μl of the kinase buffer containing 100 μM phosphatidylinositol 4-phosphate [PI(4)P] for 30 minutes at 37℃. PIP_2 formed in these assays was extracted using modified Bligh-Dyer extraction (Honeyman et al., 1983). The lipid was dissolved in chloroform/methanol (1/1, v/v) and spotted on Silicon TLC plates. The plates were developed in the solvent system: chloroform/acetone/methanol/acetic acid/water (46/17/15/14/8, v/v). PIP_2 was visualized by autoradiography and quantitated by a Beckman liquid scintillation counter.

Quantitation of polyphosphoinositides in cells

Polyphosphoinositides were extracted and derivatized using trimethylsilyl diazomethane as described (Clark et al., 2011). Polyphosphoinositides were measured as their TMS-diazomethane derivatives using a Shimadzu UFLC equipped with a Vydac 214MS C4, 5 u, 4.6×250 mm column, coupled with an ABI 4000-Qtrap hybrid linear ion trap triple quadrupole mass spectrometer in multiple reaction monitoring (MRM) mode as described previously (Wu et al., 2011).

FA dynamics assays

MDA-MB-231 cells that stably express DsRed-paxillin were infected with pBabe-ZZ-PIPKIγ90 WT, pBabe-ZZ-PIPKIγ90^{K97R} or an empty vector, and selected with neomycin (0.7 mg/ml). The cells were trypsinized and plated on MatTek dishes (with a glass coverslip at the bottom) that had been precoated with fibronectin (5 μg/ml). The cells were cultured for 3 hours and TIRF images were taken using the Nikon Eclipse Ti TIRF microscope equipped with a 60×, 1.45 NA objective, CoolSNAP HQ2 CCD camera (Roper Scientific). The temperature, CO_2 and humidity were maintained by using a INU-TIZ-F1 microscope incubation system (Tokai Hit). Images were recorded at 1-minute intervals for a 60-minute period. FA assembly and disassembly rate constants were analyzed as described previously (Webb et al., 2004; Huang et al., 2009; Wu et al., 2011).

Cell migration assays

Cells were treated with trypsin and resuspended in DMEM medium containing 1% FBS and 10 ng/ml EGF, plated at low densities on glass-bottomed dishes (MatTek) coated with 5 μg/ml fibronectin and cultured for 3 hours in a CO_2 incubator. Cell motility was measured with a Nikon Biostation IMQ. Cell migration was tracked for 6 hours; images were recorded every 10 minutes. The movement of individual cells was analyzed with NIS-Elements AR (Nikon). For Kymorgraphical analysis, images were recorded at 1-minute intervals for a 60-minute period. Protrusion persistence and velocity were analyzed as described previously (Bear et al., 2002; Huang et al., 2009).

Invasion assays

One hundred microliters of Matrigel (1:30 dilution in serum-free DMEM medium) was added to each Transwell polycarbonate filter (6 mm diameter, 8 μm pore size, Costar) and incubated with the filters at 37℃ for 6 hours. Breast cancer cells were trypsinized and washed three times with DMEM containing 1% FBS. The cells were resuspended in DMEM containing 1% FBS at a density of 5×10^5 cells/ml. The cell suspensions (100 μl) were seeded into the upper chambers, and 600 μl of DMEM medium containing 10% FBS were added to the lower chambers. The cells were allowed to invade for 12 hours (or as indicated) in a CO_2 incubator, fixed, stained and quantitated as described previously (Wu et al., 2011).

Mouse xenograft model

Animal studies were conducted in accordance with a protocol approved by the Institutional Animal Care and Use Committee at the University of Kentucky. Female ICR-SCID mice (6–8 weeks old) were maintained and treated under pathogen-free conditions. The PIPKIγ90-depleted MDA-MB-231 cells were infected with retroviruses expressing ZZ-PIPKIγ90-R or ZZ-PIPKIγ90^{K97R}-R and injected into the tail vein of mice (1×10^6 cells/mouse). After 6 weeks, mice were euthanized and lungs were removed and photographed. Tumor nodules present on the surface of lungs were examined under a dissection microscope or detected in paraffin-embedded sections stained with hematoxylin and eosin.

Acknowledgements

We thank Dr. Keith Burridge for talin antobody, Dr. Kenneth M. Yamada for his critical reading of this manuscript and Ms. Heather Spearman for her assistance with imaging analysis.

Author contributions

X.L. designed and performed experiments, interpreted data; Q.Z., M.L.K. and Z.W. performed partial experiments and analyzed data; M.S. and A.J.M. performed mass spectrometric analysis of phosphoinositides; P.R. helped with mouse experiments, H.Z. performed mass spectrometric analysis of ubiquitylation sites; B.M.E. discussed and edited the manuscript, C.H. designed experiments, interpreted data and wrote the manuscript.

Funding

This work was supported by start-up funds from Markey Cancer Center, University of Kentucky and the American Cancer Society [grant number IRG 85-001-22 to C.H.]; the National Institutes of Health [grant numbers GM0503888 and P20 GM103527-05 to A.J.M.]; and the National Institute of Dental and Craniofacial Research (NIDCR) Intramural Research Program [grant number DE000524-21 to K. Yamada for M.L.K.]. Deposited in PMC for release after 12 months.

Supplementary material available online at
http://jcs.biologists.org/lookup/suppl/doi:10.1242/jcs.117044/-/DC1

Reference

Barsukov, I. L., Prescot, A., Bate, N., Patel, B., Floyd, D. N., Bhanji, N., Bagshaw, C. R., Letinic, K., Di Paolo, G., De Camilli, P. et al. (2003). Phosphatidylinositol phosphate kinase type 1gamma and beta1-integrin cytoplasmic domain bind to the same region in the talin FERM domain. *J. Biol. Chem.* **278**, 31202-31209.

Bear, J. E., Svitkina, T. M., Krause, M., Schafer, D. A., Loureiro, J. J., Strasser, G. A., Maly, I. V., Chaga, O. Y., Cooper, J. A., Borisy, G. G. et al. (2002). Antagonism between Ena/VASP proteins and actin filament capping regulates fibroblast motility. *Cell* **109**, 509-521.

Calderwood, D. A., Tai, V., Di Paolo, G., De Camilli, P. and Ginsberg, M. H. (2004). Competition for talin results in trans-dominant inhibition of integrin activation. *J. Biol. Chem.* **279**, 28889-28895.

Chan, K. T., Bennin, D. A. and Huttenlocher, A. (2010). Regulation of adhesion dynamics by calpain-mediated proteolysis of focal adhesion kinase (FAK). *J. Biol. Chem.* **285**, 11418-11426.

Clark, E. A., Golub, T. R., Lander, E. S. and Hynes, R. O. (2000). Genomic analysis of metastasis reveals an essential role for RhoC. *Nature* **406**, 532-535.

Clark, J., Anderson, K. E., Juvin, V., Smith, T. S., Karpe, F., Wakelam, M. J. O., Stephens, L. R. and Hawkins, P. T. (2011). Quantification of PtdInsP3 molecular species in cells and tissues by mass spectrometry. *Nat. Methods* **8**, 267-272.

de Pereda, J. M., Wegener, K. L., Santelli, E., Bate, N., Ginsberg, M. H., Critchley, D. R., Campbell, I. D. and Liddington, R. C. (2005). Structural basis for phosphatidylinositol phosphate kinase type Igamma binding to talin at focal adhesions. *J. Biol. Chem.* **280**, 8381-8386.

Deakin, N. O. and Turner, C. E. (2011). Distinct roles for paxillin and Hic-5 in regulating breast cancer cell morphology, invasion, and metastasis. *Mol. Biol. Cell* **22**, 327-341.

Delorme-Walker, V. D., Peterson, J. R., Chernoff, J., Waterman, C. M., Danuser, G., DerMardirossian, C. and Bokoch, G. M. (2011). Pak1 regulates focal adhesion strength, myosin IIA distribution, and actin dynamics to optimize cell migration. *J. Cell Biol.* **193**, 1289-1303.

Di Paolo, G., Pellegrini, L., Letinic, K., Cestra, G., Zoncu, R., Voronov, S., Chang, S. H., Guo, J., Wenk, M. R. and De Camilli, P. (2002). Recruitment and regulation of phosphatidylinositol phosphate kinase type 1 gamma by the FERM domain of talin. *Nature* **420**, 85-89.

Franco, S. J., Rodgers, M. A., Perrin, B. J., Han, J. W., Bennin, D. A., Critchley, D. R. and Huttenlocher, A. (2004). Calpain-mediated proteolysis of talin regulates adhesion dynamics. *Nat. Cell Biol.* **6**, 977-983.

Gao, M., Labuda, T., Xia, Y., Gallagher, E., Fang, D., Liu, Y.-C. and Karin, M. (2004). Jun turnover is controlled through JNK-dependent phosphorylation of the E3 ligase Itch. *Science* **306**, 271-275.

Gilmore, A. P. and Burridge, K. (1996). Regulation of vinculin binding to talin and actin by phosphatidyl-inositol-4-5-bisphosphate. *Nature* **381**, 531-535.

Goksoy, E., Ma, Y.-Q., Wang, X., Kong, X., Perera, D., Plow, E. F. and Qin, J. (2008). Structural basis for the autoinhibition of talin in regulating integrin activation. *Mol. Cell* **31**, 124-133.

Goult, B. T., Bate, N., Anthis, N. J., Wegener, K. L., Gingras, A. R., Patel, B., Barsukov, I. L., Campbell, I. D., Roberts, G. C. K. and Critchley, D. R. (2009). The structure of an interdomain complex that regulates talin activity. *J. Biol. Chem.* **284**, 15097-15106.

Gupton, S. L. and Waterman-Storer, C. M. (2006). Spatiotemporal feedback between actomyosin and focal-adhesion systems optimizes rapid cell migration. *Cell* **125**, 1361-1374.

Honeyman, T. W., Strohsnitter, W., Scheid, C. R. and Schimmel, R. J. (1983). Phosphatidic acid and phosphatidylinositol labelling in adipose tissue. Relationship to the metabolic effects of insulin and insulin-like agents. *Biochem. J.* **212**, 489-498.

Huang, C. (2010). Roles of E3 ubiquitin ligases in cell adhesion and migration. *Cell Adh. Migr.* **4**, 10-18.

Huang, C. and Jacobson, K. (2010). Detection of protein-protein interactions using nonimmune IgG and BirA-mediated biotinylation. *Biotechniques* **49**, 881-886.

Huang, C., Rajfur, Z., Borchers, C., Schaller, M. D. and Jacobson, K. (2003). JNK phosphorylates paxillin and regulates cell migration. *Nature* **424**, 219-223.

Huang, C., Rajfur, Z., Yousefi, N., Chen, Z. Z., Jacobson, K. and Ginsberg, M. H. (2009). Talin phosphorylation by Cdk5 regulates Smurf1-mediated talin head ubiquitylation and cell migration. *Nat. Cell Biol.* **11**, 624-630.

Koestler, S. A., Auinger, S., Vinzenz, M., Rottner, K. and Small, J. V. (2008). Differentially oriented populations of actin filaments generated in lamellipodia collaborate in pushing and pausing at the cell front. *Nat. Cell Biol.* **10**, 306-313.

Le, P. U., Angers-Loustau, A., de Oliveira, R. M. W., Ajlan, A., Brassard, C. L., Dudley, A., Brent, H., Siu, V., Trinh, G., Mölenkamp, G. et al. (2010). DRR drives brain cancer invasion by regulating cytoskeletal-focal adhesion dynamics. *Oncogene* **29**, 4636-4647.

Lee, S. Y., Voronov, S., Letinic, K., Nairn, A. C., Di Paolo, G. and De Camilli, P. (2005). Regulation of the interaction between PIPKI gamma and talin by proline-directed protein kinases. *J. Cell Biol.* **168**, 789-799.

Legate, K. R., Takahashi, S., Bonakdar, N., Fabry, B., Boettiger, D., Zent, R. and Fässler, R. (2011). Integrin adhesion and force coupling are independently regulated by localized PtdIns(4,5)2 synthesis. *EMBO J.* **30**, 4539-4553.

Ling, K., Doughman, R. L., Firestone, A. J., Bunce, M. W. and Anderson, R. A. (2002). Type I gamma phosphatidylinositol phosphate kinase targets and regulates focal adhesions. *Nature* **420**, 89-93.

Ling, K., Doughman, R. L., Iyer, V. V., Firestone, A. J., Bairstow, S. F., Mosher, D. F., Schaller, M. D. and Anderson, R. A. (2003). Tyrosine phosphorylation of type Igamma phosphatidylinositol phosphate kinase by Src regulates an integrin-talin switch. *J. Cell Biol.* **163**, 1339-1349.

Ling, K., Schill, N. J., Wagoner, M. P., Sun, Y. and Anderson, R. A. (2006). Movin' on up: the role of PtdIns(4,5)P(2) in cell migration. *Trends Cell Biol.* **16**, 276-284.

Ling, K., Bairstow, S. F., Carbonara, C., Turbin, D. A., Huntsman, D. G. and Anderson, R. A. (2007). Type I γ phosphatidylinositol phosphate kinase modulates adherens junction and E-cadherin trafficking via a direct interaction with μ 1B adaptin. *J. Cell Biol.* **176**, 343-353.

Lokuta, M. A., Senetar, M. A., Bennin, D. A., Nuzzi, P. A., Chan, K. T., Ott, V. L. and Huttenlocher, A. (2007). Type Igamma PIP kinase is a novel uropod component that regulates rear retraction during neutrophil chemotaxis. *Mol. Biol. Cell* **18**, 5069-5080.

Lu, K., Yin, X., Weng, T., Xi, S., Li, L., Xing, G., Cheng, X., Yang, X., Zhang, L. and He, F. (2008). Targeting WW domains linker of HECT-type ubiquitin ligase Smurf1 for activation by CKIP-1. *Nat. Cell Biol.* **10**, 994-1002.

Martel, V., Racaud-Sultan, C., Dupe, S., Marie, C., Paulhe, F., Galmiche, A., Block, M. R. and Albiges-Rizo, C. (2001). Conformation, localization, and integrin binding of talin depend on its interaction with phosphoinositides. *J. Biol. Chem.* **276**, 21217-21227.

Miyazaki, T., Kato, H., Nakajima, M., Sohda, M., Fukai, Y., Masuda, N., Manda, R., Fukuchi, M., Tsukada, K. and Kuwano, H. (2003). FAK overexpression is correlated with tumour invasiveness and lymph node metastasis in oesophageal squamous cell carcinoma. *Br. J. Cancer* **89**, 140-145.

Qin, J., Xie, Y., Wang, B., Hoshino, M., Wolff, D. W., Zhao, J., Scofield, M. A., Dowd, F. J., Lin, M. F. and Tu, Y. (2009). Upregulation of PIP3-dependent Rac exchanger 1 (P-Rex1) promotes prostate cancer metastasis. *Oncogene* **28**, 1853-1863.

Ridley, A. J., Schwartz, M. A., Burridge, K., Firtel, R. A., Ginsberg, M. H., Borisy, G., Parsons, J. T. and Horwitz, A. R. (2003). Cell migration: integrating signals from front to back. *Science* **302**, 1704-1709.

Saltel, F., Mortier, E., Hytönen, V. P., Jacquier, M.-C., Zimmermann, P., Vogel, V., Liu, W. and Wehrle-Haller, B. (2009). New PI(4,5)P2- and membrane proximal integrin-binding motifs in the talin head control β3-integrin clustering. *J. Cell Biol.* **187**, 715-731.

Sarkar, A. A. and Zohn, I. E. (2012). Hectd1 regulates intracellular localization and secretion of Hsp90 to control cellular behavior of the cranial mesenchyme. *J. Cell Biol.* **196**, 789-800.

Sosa, M. S., Lopez-Haber, C., Yang, C., Wang, H., Lemmon, M. A., Busillo, J. M., Luo, J., Benovic, J. L., Klein-Szanto, A., Yagi, H. et al. (2010). Identification of the Rac-GEF P-Rex1 as an essential mediator of ErbB signaling in breast cancer. *Mol. Cell* **40**, 877-892.

Sun, Y., Ling, K., Wagoner, M. P. and Anderson, R. A. (2007). Type I γ phosphatidylinositol phosphate kinase is required for EGF-stimulated directional cell migration. *J. Cell Biol.* **178**, 297-308.

Sun, Y., Turbin, D. A., Ling, K., Thapa, N., Leung, S., Huntsman, D. G. and Anderson, R. A. (2010). Type I gamma phosphatidylinositol phosphate kinase modulates invasion and proliferation and its expression correlates with poor prognosis in breast cancer. *Breast Cancer Res.* **12**, R6.

Thapa, N., Sun, Y., Schramp, M., Choi, S., Ling, K. and Anderson, R. A. (2012). Phosphoinositide signaling regulates the exocyst complex and polarized integrin trafficking in directionally migrating cells. *Dev. Cell* **22**, 116-130.

van Rheenen, J., Song, X., van Roosmalen, W., Cammer, M., Chen, X., Desmarais, V., Yip, S.-C., Backer, J. M., Eddy, R. J. and Condeelis, J. S. (2007). EGF-induced PIP2 hydrolysis releases and activates cofilin locally in carcinoma cells. *J. Cell Biol.* **179**, 1247-1259.

Webb, D. J., Parsons, J. T. and Horwitz, A. F. (2002). Adhesion assembly, disassembly and turnover in migrating cells – over and over and over again. *Nat. Cell Biol.* **4**, E97-E100.

Webb, D. J., Donais, K., Whitmore, L. A., Thomas, S. M., Turner, C. E., Parsons, J. T. and Horwitz, A. F. (2004). FAK-Src signalling through paxillin, ERK and MLCK regulates adhesion disassembly. *Nat. Cell Biol.* **6**, 154-161.

Wu, Z., Li, X., Sunkara, M., Spearman, H., Morris, A. J. and Huang, C. (2011). PIPKIγ regulates focal adhesion dynamics and colon cancer cell invasion. *PLoS ONE* **6**, e24775.

Xu, W., Wang, P., Petri, B., Zhang, Y., Tang, W., Sun, L., Kress, H., Mann, T., Shi, Y., Kubes, P. et al. (2010a). Integrin-induced PIP5K1C kinase polarization regulates neutrophil polarization, directionality, and in vivo infiltration. *Immunity* **33**, 340-350.

Xu, Y., Bismar, T. A., Su, J., Xu, B., Kristiansen, G., Varga, Z., Teng, L., Ingber, D. E., Mammoto, A., Kumar, R. et al. (2010b). Filamin A regulates focal adhesion disassembly and suppresses breast cancer cell migration and invasion. *J. Exp. Med.* **207**, 2421-2437.

Zohn, I. E., Anderson, K. V. and Niswander, L. (2007). The Hectd1 ubiquitin ligase is required for development of the head mesenchyme and neural tube closure. *Dev. Biol.* **306**, 208-221.